

Bulk-Boundary Correspondence in Point-Gap Topological Phases

Daichi Nakamura,^{1,*} Takumi Bessho,^{2,†} and Masatoshi Sato^{1,‡}

¹*Center for Gravitational Physics and Quantum Information, Yukawa Institute for Theoretical Physics, Kyoto University, Kyoto 606-8502, Japan*

²*Corporate Research and Development Center, Toshiba Corporation, Kawasaki, Japan*



(Received 26 June 2022; revised 18 January 2024; accepted 27 February 2024; published 28 March 2024)

A striking feature of non-Hermitian systems is the presence of two different types of topology. One generalizes Hermitian topological phases, and the other is intrinsic to non-Hermitian systems, which are called line-gap topology and point-gap topology, respectively. Whereas the bulk-boundary correspondence is a fundamental principle in the former topology, its role in the latter has not been clear yet. This Letter establishes the bulk-boundary correspondence in the point-gap topology in non-Hermitian systems. After revealing the requirement for point-gap topology in the open boundary conditions, we clarify that the bulk point-gap topology in open boundary conditions can be different from that in periodic boundary conditions. On the basis of real space topological invariants and the K theory, we give a complete classification of the open boundary point-gap topology with symmetry and show that the nontrivial open boundary topology results in robust and exotic surface states.

DOI: 10.1103/PhysRevLett.132.136401

Recently, non-Hermitian topological phases have attracted much attention [1–115]. Non-Hermitian systems differ essentially from Hermitian ones: The complex-valued energy spectra of non-Hermitian systems allow two types of the gap structure, i.e., line gap and point gap [36]. Whereas the line gap is a relatively straightforward generalization of a gap in Hermitian systems, the point gap is intrinsic in non-Hermitian systems. The multiple gap structures enable corresponding topological phases of non-Hermitian systems, line-gap, and point-gap topological phases [16,36]. Both topological phases are indispensable to understanding non-Hermitian topological phenomena.

A central character of topological phases is the bulk-boundary correspondence (BBC): the bulk topology causes anomalous gapless boundary modes in the open boundary conditions (OBCs). For example, the quantum Hall systems support chiral edge modes from the nontrivial bulk Chern number [116]. The exact quantization of the Hall conductance is a consequence of the dissipationless current of the chiral edge modes.

Despite the importance, recent studies have shown that non-Hermiticity obscures the BBC [7,8,10,11,14,18–20,25,26,38,41,42,44,46,56,63,71,75,106,109]. A class of non-Hermitian systems shows completely different bulk spectra in the OBCs than in the periodic boundary conditions (PBCs). Because of this phenomenon—the *non-Hermitian skin effect* (NHSE) [18,20], the bulk energy gap in OBCs would be closed in PBCs. Therefore, a bulk topological number in PBCs can be ill defined even when a gapless boundary mode exists in a gap in OBCs. Yao and Wang [18] solved this problem in the case of line-gap

topological phases. Using the generalized Brillouin zone (GBZ) [18,19,46,63,71], they define a topological number in OBCs, and show that the new bulk topological number correctly recovers the BBC. Furthermore, later, the BBC in OBCs was also formulated in terms of real-space topological invariants, enabling the application in the study of the BBC in higher dimensions and higher-order line-gap topological phases [47,117–121].

Whereas the above prescription settled the BBC in line-gap topological phases, the BBC in point-gap topological phases has not been clear yet. In one dimension, point-gap topological numbers in PBCs result in NHSEs in OBCs, as a result of the BBC [62,64]. However, there remains uncertainty of the BBC in higher dimensions: It has been suggested that topological surface states originate from the three-dimensional winding number in PBCs [76,87,88], which is the point-gap topological number for general three-dimensional systems. Nonetheless, these surface states can disappear without changing the bulk topological number. Thus, the relation between the bulk topology and the surface states is ambiguous.

In this Letter, we establish the BBC in point-gapped topological phases. Following the strategy learned from line-gap topological phases, our arguments rely on topological numbers in OBCs. Remarkably, there appears an essentially new feature intrinsic to point-gap topological phases. We find that a particular class of non-Hermitian skin effects, which we dub in-gap skin effects, ruins point-gap topological numbers in OBCs. As a result, the topological classification in OBCs can be different from that in PBCs. Based on this result, we resolve the uncertainty of the BBC in point-gap topological phases,

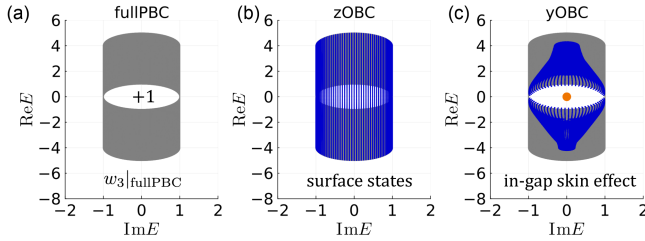


FIG. 1. The energy spectra of ETI in Eq. (1). (a) The full PBC spectrum (gray). The point gap is open around $E = 0$, with the nontrivial 3D winding number $+1$. (b) The zOBC spectrum (blue) and the full PBC spectrum (gray) in comparison. No NHSE occurs but surface states appear in the region where the 3D winding number takes the nontrivial value. The system size is $L_x = L_y = 100$ and $L_z = 30$. (c) The yOBC spectrum (blue) and the full PBC spectrum (gray) in comparison. NHSEs occur, and in-gap skin modes (orange) appear. The system size in the y direction is $L_y = 30$ and the momentum resolutions in both $k_{x,z}$ directions are taken as $\Delta k_{x,z} = 2\pi/100$.

and show that nontrivial topological numbers in OBCs result in robust and exotic surface states. Using the K theory, we also give a complete classification table for point-gap topological phases under OBCs in the presence of symmetry.

Uncertainty of BBC in point-gap topological phases.—First, let us see the forementioned uncertainty of the BBC in point-gap topological phases. We start with a model of exceptional topological insulators (ETIs) [76],

$$H_{\text{ETI}}(\mathbf{k}) = \sin k_x \sigma_x + \sin k_z \sigma_y + \left(2 - \sum_{i=x,y,z} \cos k_i\right) \sigma_z - i \sin k_y \sigma_0, \quad (1)$$

where $\sigma_{i=x,y,z}$ are the Pauli matrices and σ_0 is the 2×2 identity matrix. As shown in Fig. 1(a), the ETI has a point gap at $E = 0$ in the complex energy plane, i.e., no complex spectrum crossing the reference point $E = 0$, under PBCs in all directions (full PBC). Therefore, we can define the three-dimensional (3D) winding number over the 3D Brillouin zone (BZ) [16,36],

$$w_3|_{\text{fullPBC}} = -\frac{1}{24\pi^2} \int_{\text{BZ}} \text{Tr}[(H - E)^{-1} d(H - E)]^3, \quad (2)$$

which takes $+1$ for $H = H_{\text{ETI}}$ and $E = 0$.

Interestingly, the ETI hosts surface states once we impose the OBC in the z direction (zOBC). See Fig. 1(b). Because the non-Hermitian term $i \sin k_y \sigma_0$ in Eq. (1) only gives a complex shift of the energy under the zOBC, the surface states of the ETI are equivalent to those of a Weyl semimetal, $H_{\text{WSM}}(\mathbf{k}) = H_{\text{ETI}}(\mathbf{k}) + i \sin k_y \sigma_0 = \sin k_x \sigma_x + \sin k_z \sigma_y + (2 - \sum_{i=x,y,z} \cos k_i) \sigma_z$. For a fixed k_y with $-\pi/2 < k_y < \pi/2$, the Weyl semimetal supports a

non-zero Chern number in the PBCs, and thus it has corresponding chiral edge modes under the zOBC. By taking into account the complex energy shift from the non-Hermitian term $i \sin k_y \sigma_0$, the chiral modes give surface states filling the point-gapped region in Fig. 1(b).

These surface states have a topological number with the same value as the bulk 3D winding number: The effective Hamiltonian of the surface states around $E = 0$ takes the form of $h_{\text{surface}}(k_x, k_y) = v_x k_x - ik_y$ as the chiral edge mode of the Weyl semimetal has $v_x k_x$ with a real positive constant $v_x > 0$ and the non-Hermitian term of H_{ETI} gives $-ik_y$. The 1D winding number w_1 on a circle S^1 around $(k_x, k_y) = (0, 0)$ on the surface BZ [76]:

$$w_1 = - \oint_{S^1} \frac{d\mathbf{k}}{2\pi i} \cdot h_{\text{surface}}^{-1}(k_x, k_y) \nabla_k h_{\text{surface}}(k_x, k_y) = 1 \quad (3)$$

measures the topology of the surface states, of which value coincides with the 3D winding number.

The coincidence of the topological numbers suggests the BBC in point-gap topological phases [76]. However, there is an uncertainty in this interpretation. In Fig. 1(c), we show the spectrum of the same model under the OBC in the y direction (yOBC). Whereas the bulk topological number in Eq. (2) remains the same, no surface state covering the point-gapped region appears. Instead, we have skin modes in the gap. Since the skin modes are localized bulk modes [122], and do not have 1D winding number [64], the simple BBC does not hold under the yOBC.

Point-gap topological number under OBCs and BBC.—The solution of the problem is to use topological numbers in OBCs. Let us consider a 3D Hamiltonian $\mathcal{H}(k_x, k_y)$ with momentum-space representation in the x and y directions and real-space representation in the z direction under the zOBC. Then, we construct the bulk Hamiltonian $\mathcal{H}_{\text{bulk}}(k_x, k_y)$ by the projection of $\mathcal{H}(k_x, k_y)$ onto the bulk [47]. When the bulk Hamiltonian has a point gap at E ($\det[\mathcal{H}_{\text{bulk}} - E] \neq 0$), we can define the real-space 3D winding number w_3 under the zOBC,

$$w_3|_{\text{zOBC}} = -\frac{i}{12\pi} \int_{\text{BZ}} d^2\mathbf{k} \mathcal{T}_z[e^{ijk} Q_i Q_j Q_k], \quad (4)$$

with $Q_{i=x,y} = i(\mathcal{H}_{\text{bulk}} - E)^{-1} \partial_{k_i} (\mathcal{H}_{\text{bulk}} - E)$ and $Q_z = (\mathcal{H}_{\text{bulk}} - E)^{-1} [Z, \mathcal{H}_{\text{bulk}} - E]$, where Z is the position operator in the z coordinate, and \mathcal{T}_z stands for the trace per unit length in the z direction. This is a non-Hermitian generalization of the real-space topological number in Hermitian systems [123–126]. For the full PBCs, this quantity reproduces Eq. (2) with the identification

$$\int \frac{dk_z}{2\pi} \text{Tr}[A(k_z)] \leftrightarrow \mathcal{T}_z[\mathcal{A}], \quad i\partial_{k_z} \leftrightarrow [Z, \cdot], \quad (5)$$

where $A(k_z)$ is a function of k_z and \mathcal{A} is the real-space representation of $A(k_z)$ [127,128]. Thus, for the ETI in

Eq. (1), the coincidence between $w_3|_{\text{fullPBC}}$ with $E = 0$ in Eq. (2) and w_1 in Eq. (3) results in the correspondence between $w_3|_{\text{zOBC}}$ with $E = 0$ in Eq. (4) and w_1 in Eq. (3). Since any nontrivial 3D winding number under zOBC can be produced by stacking the ETIs in Eq. (1) up to continuous deformations, we generally have the BBC

$$w_3|_{\text{zOBC}} = \sum_{\mathbf{k}_p} w_1(\mathbf{k}_p), \quad (6)$$

with

$$w_1(\mathbf{k}_p) = - \oint_{S_p^1} \frac{d\mathbf{k}}{2\pi i} \cdot \text{Tr}[(h_{\text{surface}} - E)^{-1} \nabla(h_{\text{surface}} - E)], \quad (7)$$

where $h_{\text{surface}}(k_x, k_y)$ is the surface effective Hamiltonian, \mathbf{k}_p is the Fermi point satisfying $\det[h_{\text{surface}}(\mathbf{k}_p) - E] = 0$, and S_p^1 stands for the counterclockwise circle around $\mathbf{k} = \mathbf{k}_p$ on the surface Brillouin zone. As we shall show later, the bulk topological number under the zOBC can be different from that under the yOBC. Therefore, the above BBC does not require surface states under the yOBC.

The necessity of the OBC bulk topological number becomes obvious once we consider another model. Figure 2(a) is the bulk spectra of the following model under different boundary conditions:

$$H(\mathbf{k}) = \sin k_x \sigma_x + 2 \sin k_z \sigma_y + 2 \left(2 - \sum_{i=x,y,z} \cos k_i \right) \sigma_z + \frac{3}{2} i (\sin k_y + \sin k_z) \sigma_0. \quad (8)$$

Because of NHSEs in the bulk spectrum, the OBC spectrum has a wider point-gapped region than the PBC spectrum. Therefore, there is a region where only the topological number under the zOBC is well defined, as shown in Fig. 2. We find that the BBC holds for the topological number under the zOBC, not for that under the PBC.

In-gap skin effects and absence of surface states.—Now we show that the BBC in Eq. (6) also explains the absence of surface states in Fig. 1(c) under the yOBC. A key observation is the presence of in-gap skin modes. In a manner similar to Eq. (4), we can introduce the 3D winding number under the yOBC, but the in-gap bulk skin modes make the topological number ill defined. Consequently, the BBC under the yOBC does not require any surface states.

Let us see how this happens in detail. First, we note that the in-gap skin modes originate from modes with $(k_x, k_z) = (0, 0)$, where the Hamiltonian in Eq. (1) becomes

$$H_{\text{ETI}}(k_x = 0, k_y, k_z = 0) = -\cos k_y \sigma_z - i \sin k_y \sigma_0. \quad (9)$$

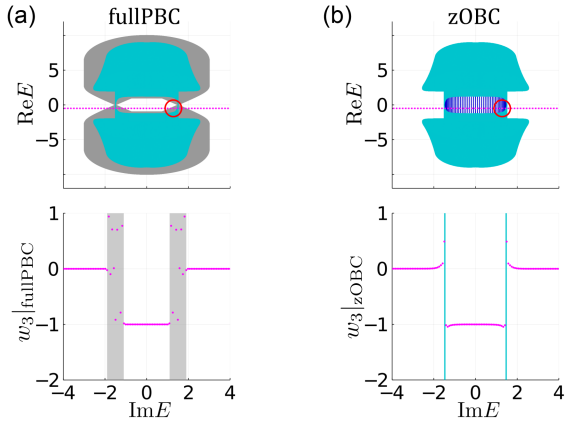


FIG. 2. The energy spectra (top) and the 3D winding numbers (bottom) of the model in Eq. (8) under different boundary conditions. The magenta lines in the top figures represent $E = -0.5 + i\text{Im}E$ with $-4 < \text{Im}E < 4$. (a) (top) The bulk spectra under the full PBC (gray) and the zOBC (turquoise). The zOBC spectrum is calculated by using the non-Bloch theory in Ref. [46]. The point-gapless region under the zOBC is wider than that under the full PBCs. (bottom) The 3D winding number under the full PBC along the magenta line in the top figure. The gray shadings represent point-gapless regions. (b) (top) The energy spectrum under the zOBC. The blue modes are surface states which are calculated with the system size $L_x = L_y = 100, L_z = 20$. Surface states appear even in the regions where $w_3|_{\text{fullPBC}}$ is ill defined (inside the red circle). (bottom) The real-space 3D winding number under the zOBC along the magenta line in the top figure. The turquoise segments represent point-gapless regions.

This 1D Hamiltonian gives the complex spectra $\mp e^{\pm ik_y}$ in the eigensector of $\sigma_z = \pm 1$, which have the energy winding numbers ± 1 along the k_y direction, as illustrated in Fig. 3(a). Thus, from the general theory of NHSE [64], we have the skin modes inside the point gap when one imposes the yOBC [129].

At first glance, the in-gap skin modes appear to be isolated from the other bulk modes, but this is not the case. For a finite L_y , the Hamiltonian under the yOBC is a continuous function with respect to k_x and k_z , so is its eigenvalues. Therefore, there must be ordinary bulk modes nearby the skin modes. Figure 3(c) shows the energy spectrum of Eq. (1) under the yOBC, with a high momentum resolution. The bulk modes around the in-gap skin modes are now evident. Importantly, the point-gapped region disappears due to these bulk modes. Therefore, we do not have a well-defined 3D winding number and surface states under the yOBC.

The disappearance of surface modes can be regarded as a result of a topological phase transition under continuous change of the boundary conditions. Decreasing the hopping terms between the $y = 1$ sites and $y = L_y$ sites, we can smoothly change the boundary condition from the full PBC to the yOBC. According to the deformation, the modes at $(k_x, k_z) = (0, 0)$ shrink to the in-gap skin modes as shown

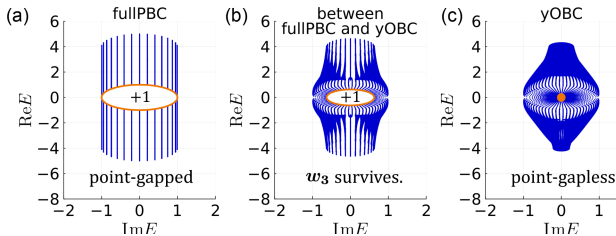


FIG. 3. The changes of the spectra of ETI in Eq. (1) from under the full PBC to the yOBC. L_y is the same as that in Fig. 1(c) but the momentum resolution around $(k_x, k_z) = (0, 0)$ is much finer. The orange modes represent the modes with $k_x = k_z = 0$. (a) The full PBC spectrum. A point gap is open in the region containing $E = 0$ with the nontrivial 3D winding number +1. The modes at $k_x = k_z = 0$ form a loop and have a nontrivial 1D winding number in each eigensector of $\sigma_z = \pm 1$. (b) The spectrum under a boundary condition between the $y = 1$ sites and the $y = L_y$ sites is 10^{-6} . The point-gapped region with the nonzero 3D winding number shrinks. (c) The yOBC spectrum. The region including $E = 0$ is completely closed by the in-gap skin effect of the modes at $k_x = k_z = 0$. Comparing with Fig. 1(c), we can see that the point-gapped region is completely collapsed by the modes near $k_x = k_z = 0$.

in Fig. 3(b). Finally, the originally point-gapped region is fully covered by bulk modes under the yOBC. We also show the change of the 3D winding number throughout the topological phase transition for the model in Eq. (8) in the Supplemental Material [130].

BBC of point-gap topology with symmetry.—The above arguments can also apply to point-gapped systems under symmetries. Namely, when a symmetry-protected point-gap topological number under the OBC is nonzero, then the corresponding boundary states appear.

It should be noted here that possible point-gap topological numbers under OBCs can be different from those under PBCs. The disagreement stems from the property that some point-gap topological numbers in PBCs are always accompanied by in-gap skin modes, which spoil the corresponding topological numbers in OBCs.

Whereas we have considered the full general symmetries in the Supplemental Material [130], we focus here on a particular class of symmetries, which we call AZ[†] symmetry. The AZ[†] symmetries are a non-Hermitian generalization of the Altland-Zirnbauer (AZ) symmetry [36]: It consists of non-Hermitian versions of time-reversal symmetry (TRS[†]), $C\mathcal{H}^T(\mathbf{k})\mathcal{C}^{-1} = H(-\mathbf{k})$, particle-hole symmetry (PHS[†]), $T\mathcal{H}^*(\mathbf{k})T^{-1} = -H(-\mathbf{k})$, and chiral symmetry (CS) $\Gamma H^\dagger(\mathbf{k})\Gamma^{-1} = -H(\mathbf{k})$, where \mathcal{C} , T , and Γ are unitary operators. The AZ[†] symmetry naturally arises in the non-Hermitian Hamiltonian of the retarded Green's function, and thus it governs non-Hermitian topological phases in materials [135]. The presence and/or absence of these symmetries define ten symmetry classes, and the topological classification in these classes under the full PBC has been known [36].

TABLE I. Classification of point-gap topological phases. For topological numbers with arrows, the left specifies topological numbers under PBCs and the right specifies those under OBCs. For topological numbers without arrows, the classification under OBCs coincides with that under PBCs. We consider the AZ[†] symmetry classes with the spatial dimension $d = 1, 2$, and 3.

Symmetry class	TRS [†]	PHS [†]	CS	$d = 1$	$d = 2$	$d = 3$
A	0	0	0	$\mathbb{Z} \rightarrow 0$	0	\mathbb{Z}
AIII	0	0	1	0	\mathbb{Z}	0
AI [†]	+1	0	0	0	0	$2\mathbb{Z}$
BDI [†]	+1	+1	1	0	0	0
D [†]	0	+1	0	$\mathbb{Z} \rightarrow 0$	0	0
DIII [†]	-1	+1	1	$\mathbb{Z}_2 \rightarrow 0$	$\mathbb{Z} \rightarrow 2\mathbb{Z}$	0
AII [†]	-1	0	0	$\mathbb{Z}_2 \rightarrow 0$	$\mathbb{Z}_2 \rightarrow 0$	$\mathbb{Z} \rightarrow 2\mathbb{Z}$
CII [†]	-1	-1	1	0	\mathbb{Z}_2	\mathbb{Z}_2
C [†]	0	-1	0	$2\mathbb{Z} \rightarrow 0$	0	\mathbb{Z}_2
CI [†]	+1	-1	1	0	$2\mathbb{Z}$	0

In Table I, we show how the point-gap topological classification under the PBCs changes under OBCs: In one dimension, all the point-gap topological numbers in the AZ[†] classes become trivial under the OBC, because their nontrivial values in the PBC always result in in-gap skin modes under the OBC. Actually, all the \mathbb{Z} indices in 1D AZ[†] classes reduce to the 1D winding number [36], which gives in-gap skin modes under the OBC [62,64]. Furthermore, the \mathbb{Z}_2 topological number in 1D classes AII[†] and DIII[†] under the PBC causes symmetry-protected skin modes inside the point gap under the OBC [64]. Therefore, no 1D point-gap topological number survives under the OBC.

The reduction of topological numbers in Table I in two and three dimensions occurs as a result of the dimensional reduction [136]. First, we focus on class AII[†]. From a Hamiltonian $H(\mathbf{k})$ with a point gap at E in class AII[†], we can obtain a topologically equivalent gapped Hermitian Hamiltonian $\tilde{H}(\mathbf{k})$:

$$\tilde{H}(\mathbf{k}) = \begin{pmatrix} 0 & H(\mathbf{k}) - E \\ H^\dagger(\mathbf{k}) - E^* & 0 \end{pmatrix}, \quad (10)$$

which belongs to class DIII as it has an additional CS $\Sigma \tilde{H}(\mathbf{k}) \Sigma^{-1} = -\tilde{H}(\mathbf{k})$ ($\Sigma = \sigma_z \otimes 1$) together with TRS $\tilde{\mathcal{C}} \tilde{H}^*(\mathbf{k}) \tilde{\mathcal{C}}^{-1} = \tilde{H}(-\mathbf{k})$ ($\tilde{\mathcal{C}} = \sigma_x \otimes \mathcal{C}$) [36]. Using the dimensional reduction in class DIII [136], one can show that the parity of the 3D \mathbb{Z} index for $H(k_x, k_y, k_z)$ equals to the product of the 2D \mathbb{Z}_2 indices of $H(k_x, k_y, k_z^0)$ with $k_z^0 = 0$ and π , and similarly, the 2D \mathbb{Z}_2 index of $H(k_x, k_y, k_z^0)$ equals to the product of the 1D \mathbb{Z}_2 indices of $H(k_x, k_y^0, k_z^0)$ with $k_y^0 = 0$ and π . Thus, for class AII[†] under full PBCs, a non-trivial 2D \mathbb{Z}_2 index or an odd parity of the 3D \mathbb{Z} index at E yield a nonzero 1D \mathbb{Z}_2 index at E along a high

symmetric line in the BZ. Therefore, they always accompany symmetry-protected in-gap skin modes [64], trivializing the corresponding topological numbers in OBCs. As a result, only the even part of the \mathbb{Z} index in three dimensions survives in the OBC. We can also show the reduction $\mathbb{Z} \rightarrow 2\mathbb{Z}$ in 2D class DIII † , using a similar dimensional reduction. On the basis of the K theory, we prove the BBC for point-gap topological phases under the OBC in all 38-fold symmetry classes in non-Hermitian systems, including AZ † ones, in the Supplemental Material [130].

Remarkably, we can predict novel topological phase transitions intrinsic to non-Hermitian systems, using the reduction of the point-gap topological numbers in the presence of symmetry: The symmetry-protected in-gap skin modes in 3D class AII † systems may disappear suddenly once one breaks TRS † by an infinitesimal perturbation. The disappearance of the in-gap skin modes allows the well-defined 3D winding number under the OBC, and thus we have an abrupt transmutation from the topologically trivial state with the in-gap skin modes to a topologically nontrivial one with surface states. Infinitesimal instability [49] intrinsic to non-Hermitian systems induces this topological phase transition, and thus it never happens in Hermitian systems. We also find that boundary states in intrinsic point-gap topological phases may support a single exceptional point [130], which is also unique to non-Hermitian systems.

Conclusions.—In this Letter, we establish the BBC for the point-gap topology in non-Hermitian systems. We demonstrate that real-space topological numbers under OBCs result in robust and exotic surface states. We find that the bulk point-gap topology in OBCs can be different from that in PBCs, and give a complete classification of the OBC point-gap topology in the presence of symmetry. Our finding reveals a novel universal property of non-Hermitian topological phases of matters.

We are grateful to Nobuyuki Okuma, Ken Shiozaki, Shuhei Ohyama, Yusuke Nakai, and Hiroto Oka for valuable discussions. This work was supported by JST CREST Grant No. JPMJCR19T2, the establishment of university fellowships towards the creation of science technology innovation, Grant No. JPMJFS2123, KAKENHI Grant No. JP21J11810, and KAKENHI Grant No. JP20H00131. This work was done while Takumi Bessho was at Yukawa Institute for Theoretical Physics, Kyoto University.

Appendix on the BBC for point-gap topological phases in general symmetry classes.—Our argument is applicable to any symmetry classes in non-Hermitian systems. We summarize here our results for point-gap topological phases in general symmetry classes in non-Hermitian systems. For the details of the derivation, see Supplemental Material [130].

TABLE II. AZ and AZ † symmetry classes for non-Hermitian Hamiltonians. Here, “0” denotes the absence of symmetries, while “ ± 1 ” indicates the presence of each symmetry, dependent on whether its operator squares to ± 1 .

Symmetry class		TRS	PHS	CS	TRS †	PHS †
Complex AZ	A	0	0	0	0	0
	AIII	0	0	1	0	0
Real AZ	AI	+1	0	0	0	0
	BDI	+1	+1	1	0	0
	D	0	+1	0	0	0
	DIII	-1	+1	1	0	0
	AII	-1	0	0	0	0
	CII	-1	-1	1	0	0
	C	0	-1	0	0	0
	CI	+1	-1	1	0	0
Real AZ †	AI †	0	0	0	+1	0
	BDI †	0	0	1	+1	+1
	D †	0	0	0	0	+1
	DIII †	0	0	1	-1	+1
	AII †	0	0	0	-1	0
	CII †	0	0	1	-1	-1
	C †	0	0	0	0	-1
	CI †	0	0	1	+1	-1

In addition to AZ † symmetries discussed in the main text, non-Hermitian systems allow the original AZ symmetries defined by the following equations:

$$\begin{aligned} TH^*(\mathbf{k})\mathcal{T}^{-1} &= H(-\mathbf{k}), & \mathcal{T}\mathcal{T}^* &= \pm 1, \\ CH^T(\mathbf{k})\mathcal{C}^{-1} &= -H(-\mathbf{k}), & \mathcal{C}\mathcal{C}^* &= \pm 1, \end{aligned} \quad (\text{A1})$$

where \mathcal{T} and \mathcal{C} are unitary operators corresponding to time-reversal symmetry (TRS) and particle-hole symmetry (PHS), respectively. Furthermore, as an additional general symmetry, one can also introduce sublattice symmetry (SLS),

$$SH(\mathbf{k})\mathcal{S}^{-1} = -H(\mathbf{k}), \quad \mathcal{S}^2 = 1, \quad (\text{A2})$$

or pseudo-Hermiticity (pH)

$$\eta H^\dagger(\mathbf{k})\eta^{-1} = H(\mathbf{k}), \quad \eta^2 = 1 \quad (\text{A3})$$

with unitary operators \mathcal{S} and η . The presence and/or absence of these symmetries define symmetry classes intrinsic to non-Hermitian systems [36].

Tables III and IV summarize our results on point-gap topological phases in general symmetry classes. Here, the presence or absence of AZ or AZ † symmetries define AZ or AZ † symmetry classes in Table II. Moreover, each AZ or AZ † class can host SLS (pH) additionally, where the subindex $+(-)$ of \mathcal{S}/η in Tables III and IV specifies the

TABLE III. Classification of point-gap topological phases in the AZ classes without or with SLS or pH. The subscript of $\mathcal{S}_{\pm}/\eta_{\pm}$ specifies the commutation (+) or anticommutation (-) relation to TRS or PHS. For $\mathcal{S}_{\pm\pm}/\eta_{\pm\pm}$, the first subscript specifies the relation to TRS and the second specifies the relation to PHS. For the topological numbers with arrows, the classification under OBCs changes from that under PBCs, where the left specifies the classification under PBCs and the right specifies that under OBCs. The topological number $\mathbb{Z}[i, j]$ ($\mathbb{Z}_2[i, j]$) under OBCs indicates the Abelian group \mathbb{Z} (\mathbb{Z}_2) generated by the element $(i, j) \in \mathbb{Z} \oplus \mathbb{Z}$ [$(i, j) \in \mathbb{Z}_2 \oplus \mathbb{Z}_2$] under PBCs. For the topological numbers without arrows, the classification under OBCs coincides with that under PBCs.

AZ class	Additional symmetry	$d = 1$	$d = 2$	$d = 3$
A	...	$\mathbb{Z} \rightarrow 0$	0	\mathbb{Z}
AI	...	\mathbb{Z}_2	\mathbb{Z}_2	\mathbb{Z}_2
AI	\mathcal{S}	$\mathbb{Z} \oplus \mathbb{Z} \rightarrow \mathbb{Z}[1, -1]$	0	$\mathbb{Z} \oplus \mathbb{Z}$
AI	\mathcal{S}_{-, η_-}	0	$\mathbb{Z} \oplus \mathbb{Z}$	0
AII	η	0	\mathbb{Z}	0
AII	\mathcal{S}_{+, η_+}	\mathbb{Z}	0	\mathbb{Z}
AI	...	$\mathbb{Z} \rightarrow 0$	0	0
BDI	...	\mathbb{Z}_2	\mathbb{Z}	0
D	...	\mathbb{Z}_2	\mathbb{Z}_2	\mathbb{Z}
DIII	...	0	\mathbb{Z}_2	\mathbb{Z}_2
AII	...	$2\mathbb{Z} \rightarrow 0$	0	\mathbb{Z}_2
CII	...	0	$2\mathbb{Z}$	0
C	...	0	0	$2\mathbb{Z}$
CI	...	0	0	0
AI	\mathcal{S}_+	$\mathbb{Z} \oplus \mathbb{Z} \rightarrow \mathbb{Z}[1, -1]$	0	0
BDI	$\mathcal{S}_{+-}, \eta_{-+}$	$\mathbb{Z}_2 \oplus \mathbb{Z}_2 \rightarrow \mathbb{Z}_2[1, 1]$	$\mathbb{Z} \oplus \mathbb{Z} \rightarrow \mathbb{Z}[2, 0] \oplus \mathbb{Z}[1, -1]$	0
D	\mathcal{S}_-	$\mathbb{Z}_2 \oplus \mathbb{Z}_2 \rightarrow \mathbb{Z}_2[1, 1]$	$\mathbb{Z}_2 \oplus \mathbb{Z}_2 \rightarrow \mathbb{Z}_2[1, 1]$	$\mathbb{Z} \oplus \mathbb{Z} \rightarrow \mathbb{Z}[2, 0] \oplus \mathbb{Z}[1, -1]$
DIII	$\mathcal{S}_{+-}, \eta_{+-}$	0	$\mathbb{Z}_2 \oplus \mathbb{Z}_2$	$\mathbb{Z}_2 \oplus \mathbb{Z}_2$
AII	\mathcal{S}_+	$2\mathbb{Z} \oplus 2\mathbb{Z} \rightarrow 2\mathbb{Z}[1, -1]$	0	$\mathbb{Z}_2 \oplus \mathbb{Z}_2$
CII	$\mathcal{S}_{+-}, \eta_{-+}$	0	$2\mathbb{Z} \oplus 2\mathbb{Z}$	0
C	\mathcal{S}_-	0	0	$2\mathbb{Z} \oplus 2\mathbb{Z}$
CI	$\mathcal{S}_{+-}, \eta_{+-}$	0	0	0
AI	\mathcal{S}_-	$\mathbb{Z} \rightarrow 0$	0	\mathbb{Z}
BDI	$\mathcal{S}_{-+}, \eta_{+-}$	0	\mathbb{Z}	0
D	\mathcal{S}_+	\mathbb{Z}	0	\mathbb{Z}
DIII	$\mathcal{S}_{-+}, \eta_{-+}$	0	\mathbb{Z}	0
AII	\mathcal{S}_-	$\mathbb{Z} \rightarrow 0$	0	\mathbb{Z}
CII	$\mathcal{S}_{-+}, \eta_{+-}$	0	\mathbb{Z}	0
C	\mathcal{S}_+	$\mathbb{Z} \rightarrow 2\mathbb{Z}$	0	\mathbb{Z}
CI	$\mathcal{S}_{-+}, \eta_{-+}$	0	\mathbb{Z}	0
AI	η_+	0	0	0
BDI	$\mathcal{S}_{++}, \eta_{++}$	\mathbb{Z}	0	0
D	η_+	\mathbb{Z}_2	\mathbb{Z}_2	0
DIII	$\mathcal{S}_{--}, \eta_{++}$	\mathbb{Z}_2	\mathbb{Z}_2	\mathbb{Z}
AII	η_+	0	\mathbb{Z}_2	\mathbb{Z}_2
CII	$\mathcal{S}_{++}, \eta_{++}$	$2\mathbb{Z}$	0	\mathbb{Z}_2
C	η_+	0	$2\mathbb{Z}$	0
CI	$\mathcal{S}_{--}, \eta_{++}$	0	0	$2\mathbb{Z}$
AI	η_-	$\mathbb{Z}_2 \rightarrow 0$	$\mathbb{Z} \rightarrow 2\mathbb{Z}$	0
BDI	$\mathcal{S}_{--, \eta_{--}}$	\mathbb{Z}_2	\mathbb{Z}_2	\mathbb{Z}
D	η_-	0	\mathbb{Z}_2	\mathbb{Z}_2
DIII	$\mathcal{S}_{++, \eta_{--}}$	$2\mathbb{Z}$	0	\mathbb{Z}_2
AII	η_-	0	$2\mathbb{Z}$	0
CII	$\mathcal{S}_{--, \eta_{--}}$	0	0	$2\mathbb{Z}$
C	η_-	0	0	0
CI	$\mathcal{S}_{++, \eta_{--}}$	$\mathbb{Z} \rightarrow 2\mathbb{Z}$	0	0

TABLE IV. Classification of point-gap topological phases in the real AZ^\dagger classes without or with SLS or pH. The subscript of $\mathcal{S}_{\pm}/\eta_{\pm}$ specifies the commutation (+) or anticommutation (-) relation to TRS^\dagger or PHS^\dagger . For $\mathcal{S}_{\pm\pm}/\eta_{\pm\pm}$, the first subscript specifies the relation to TRS^\dagger and the second specifies the relation to PHS^\dagger . For the topological numbers with arrows, the classification under OBCs changes from that under PBCs, where the left specifies the classification under PBCs and the right specifies that under OBCs. The topological number $\mathbb{Z}[i, j]$ ($\mathbb{Z}_2[i, j]$) under OBCs indicates the Abelian group \mathbb{Z} (\mathbb{Z}_2) generated by the element $(i, j) \in \mathbb{Z} \oplus \mathbb{Z} [(i, j) \in \mathbb{Z}_2 \oplus \mathbb{Z}_2]$ under PBCs. For the topological numbers without arrows, the classification under OBCs coincides with that under PBCs.

AZ^\dagger class	Additional symmetry	$d = 1$	$d = 2$	$d = 3$
AI †	...	0	0	$2\mathbb{Z}$
BDI †	...	0	0	0
D †	...	$\mathbb{Z} \rightarrow 0$	0	0
DIII †	...	$\mathbb{Z}_2 \rightarrow 0$	$\mathbb{Z} \rightarrow 2\mathbb{Z}$	0
AII †	...	$\mathbb{Z}_2 \rightarrow 0$	$\mathbb{Z}_2 \rightarrow 0$	$\mathbb{Z} \rightarrow 2\mathbb{Z}$
CII †	...	0	\mathbb{Z}_2	\mathbb{Z}_2
C †	...	$2\mathbb{Z} \rightarrow 0$	0	\mathbb{Z}_2
CI †	...	0	$2\mathbb{Z}$	0
AI †	\mathcal{S}_+	\mathbb{Z}	0	\mathbb{Z}
BDI †	$\mathcal{S}_{+-}, \eta_{-+}$	0	\mathbb{Z}	0
D †	\mathcal{S}_-	$\mathbb{Z} \rightarrow 0$	0	\mathbb{Z}
DIII †	$\mathcal{S}_{+-}, \eta_{+-}$	0	\mathbb{Z}	0
AII †	\mathcal{S}_+	$\mathbb{Z} \rightarrow 2\mathbb{Z}$	0	\mathbb{Z}
CII †	$\mathcal{S}_{+-}, \eta_{-+}$	0	\mathbb{Z}	0
C †	\mathcal{S}_-	$\mathbb{Z} \rightarrow 0$	0	\mathbb{Z}
CI †	$\mathcal{S}_{+-}, \eta_{+-}$	0	\mathbb{Z}	0
AI †	\mathcal{S}_-	0	0	$2\mathbb{Z} \oplus 2\mathbb{Z}$
BDI †	$\mathcal{S}_{-+}, \eta_{+-}$	0	0	0
D †	\mathcal{S}_+	$\mathbb{Z} \oplus \mathbb{Z} \rightarrow \mathbb{Z}[1, -1]$	0	0
DIII †	$\mathcal{S}_{-+}, \eta_{-+}$	$\mathbb{Z}_2 \oplus \mathbb{Z}_2 \rightarrow \mathbb{Z}_2[1, 1]$	$\mathbb{Z} \oplus \mathbb{Z} \rightarrow \mathbb{Z}[2, 0] \oplus \mathbb{Z}[1, -1]$	0
AII †	\mathcal{S}_-	$\mathbb{Z}_2 \oplus \mathbb{Z}_2 \rightarrow \mathbb{Z}_2[1, 1]$	$\mathbb{Z}_2 \oplus \mathbb{Z}_2 \rightarrow \mathbb{Z}_2[1, 1]$	$\mathbb{Z} \oplus \mathbb{Z} \rightarrow \mathbb{Z}[2, 0] \oplus \mathbb{Z}[1, -1]$
CII †	$\mathcal{S}_{-+}, \eta_{+-}$	0	$\mathbb{Z}_2 \oplus \mathbb{Z}_2$	$\mathbb{Z}_2 \oplus \mathbb{Z}_2$
C †	\mathcal{S}_+	$2\mathbb{Z} \oplus 2\mathbb{Z} \rightarrow 2\mathbb{Z}[1, -1]$	0	$\mathbb{Z}_2 \oplus \mathbb{Z}_2$
CI †	$\mathcal{S}_{-+}, \eta_{-+}$	0	$2\mathbb{Z} \oplus 2\mathbb{Z}$	0
AI †	η_+	\mathbb{Z}_2	\mathbb{Z}	0
BDI †	$\mathcal{S}_{++}, \eta_{++}$	\mathbb{Z}	0	0
D †	η_+	0	0	0
DIII †	$\mathcal{S}_{--}, \eta_{++}$	\mathbb{Z}_2	\mathbb{Z}_2	\mathbb{Z}
AII †	η_+	0	$2\mathbb{Z}$	0
CII †	$\mathcal{S}_{++}, \eta_{++}$	$2\mathbb{Z}$	0	\mathbb{Z}_2
C †	η_+	0	\mathbb{Z}_2	\mathbb{Z}_2
CI †	$\mathcal{S}_{--}, \eta_{++}$	0	0	$2\mathbb{Z}$
AI †	η_-	0	\mathbb{Z}_2	\mathbb{Z}_2
BDI †	$\mathcal{S}_{--}, \eta_{--}$	0	0	$2\mathbb{Z}$
D †	η_-	$\mathbb{Z}_2 \rightarrow 0$	$\mathbb{Z} \rightarrow 2\mathbb{Z}$	0
DIII †	$\mathcal{S}_{++}, \eta_{--}$	$\mathbb{Z} \rightarrow 2\mathbb{Z}$	0	0
AII †	η_-	0	0	0
CII †	$\mathcal{S}_{--}, \eta_{--}$	\mathbb{Z}_2	\mathbb{Z}_2	\mathbb{Z}
C †	η_-	0	$2\mathbb{Z}$	0
CI †	$\mathcal{S}_{++}, \eta_{--}$	$2\mathbb{Z}$	0	\mathbb{Z}_2

commutation (anticommutation) relation between SLS/pH and AZ or AZ^\dagger symmetries. For an AZ (AZ^\dagger) class having both TRS (TRS^\dagger) and PHS (PHS^\dagger), \mathcal{S} or η has a double subindex, where the first index specifies the commutation

or anticommutation relation between SLS and TRS (TRS^\dagger), and the second one specifies those between SLS and PHS (PHS^\dagger), respectively. Tables III and IV show how the point-gap topological classification under the PBCs changes

under OBCs. For the topological numbers with arrows, the classification under the PBCs shown on the left changes to that under OBCs on the right, while the topological numbers without arrows remain the same under both boundary conditions. We also find that the BBC holds for the point-gap topological classification under OBCs: Topologically protected boundary states appear when the bulk point-gap topological numbers under OBCs are nontrivial.

*daichi.nakamura@yukawa.kyoto-u.ac.jp

[†]takumi1.bessho@toshiba.co.jp

[‡]msato@yukawa.kyoto-u.ac.jp

- [1] M. S. Rudner and L. S. Levitov, *Phys. Rev. Lett.* **102**, 065703 (2009).
- [2] M. Sato, K. Hasebe, K. Esaki, and M. Kohmoto, *Prog. Theor. Phys.* **127**, 937 (2012).
- [3] K. Esaki, M. Sato, K. Hasebe, and M. Kohmoto, *Phys. Rev. B* **84**, 205128 (2011).
- [4] Y. C. Hu and T. L. Hughes, *Phys. Rev. B* **84**, 153101 (2011).
- [5] H. Schomerus, *Opt. Lett.* **38**, 1912 (2013).
- [6] S. Malzard, C. Poli, and H. Schomerus, *Phys. Rev. Lett.* **115**, 200402 (2015).
- [7] T. E. Lee, *Phys. Rev. Lett.* **116**, 133903 (2016).
- [8] D. Leykam, K. Y. Bliokh, C. Huang, Y. D. Chong, and F. Nori, *Phys. Rev. Lett.* **118**, 040401 (2017).
- [9] Y. Xu, S.-T. Wang, and L.-M. Duan, *Phys. Rev. Lett.* **118**, 045701 (2017).
- [10] Y. Xiong, *J. Phys. Commun.* **2**, 035043 (2018).
- [11] H. Shen, B. Zhen, and L. Fu, *Phys. Rev. Lett.* **120**, 146402 (2018).
- [12] V. Kozii and L. Fu, [arXiv:1708.05841](#).
- [13] K. Takata and M. Notomi, *Phys. Rev. Lett.* **121**, 213902 (2018).
- [14] V. M. Martinez Alvarez, J. E. Barrios Vargas, and L. E. F. Foa Torres, *Phys. Rev. B* **97**, 121401(R) (2018).
- [15] K. Kawabata, Y. Ashida, H. Katsura, and M. Ueda, *Phys. Rev. B* **98**, 085116 (2018).
- [16] Z. Gong, Y. Ashida, K. Kawabata, K. Takasan, S. Higashikawa, and M. Ueda, *Phys. Rev. X* **8**, 031079 (2018).
- [17] K. Kawabata, S. Higashikawa, Z. Gong, Y. Ashida, and M. Ueda, *Nat. Commun.* **10**, 297 (2019).
- [18] S. Yao and Z. Wang, *Phys. Rev. Lett.* **121**, 086803 (2018).
- [19] S. Yao, F. Song, and Z. Wang, *Phys. Rev. Lett.* **121**, 136802 (2018).
- [20] F. K. Kunst, E. Edvardsson, J. C. Budich, and E. J. Bergholtz, *Phys. Rev. Lett.* **121**, 026808 (2018).
- [21] K. Kawabata, K. Shiozaki, and M. Ueda, *Phys. Rev. B* **98**, 165148 (2018).
- [22] A. McDonald, T. Pereg-Barnea, and A. A. Clerk, *Phys. Rev. X* **8**, 041031 (2018).
- [23] J. Carlström and E. J. Bergholtz, *Phys. Rev. A* **98**, 042114 (2018).
- [24] J. Carlström, M. Stålhammar, J. C. Budich, and E. J. Bergholtz, *Phys. Rev. B* **99**, 161115(R) (2019).
- [25] C. H. Lee and R. Thomale, *Phys. Rev. B* **99**, 201103(R) (2019).
- [26] L. Jin and Z. Song, *Phys. Rev. B* **99**, 081103(R) (2019).
- [27] J. C. Budich, J. Carlström, F. K. Kunst, and E. J. Bergholtz, *Phys. Rev. B* **99**, 041406(R) (2019).
- [28] R. Okugawa and T. Yokoyama, *Phys. Rev. B* **99**, 041202(R) (2019).
- [29] T. Liu, Y.-R. Zhang, Q. Ai, Z. Gong, K. Kawabata, M. Ueda, and F. Nori, *Phys. Rev. Lett.* **122**, 076801 (2019).
- [30] T. Yoshida, R. Peters, N. Kawakami, and Y. Hatsugai, *Phys. Rev. B* **99**, 121101(R) (2019).
- [31] H. Zhou, J. Y. Lee, S. Liu, and B. Zhen, *Optica* **6**, 190 (2019).
- [32] C. H. Lee, L. Li, and J. Gong, *Phys. Rev. Lett.* **123**, 016805 (2019).
- [33] F. K. Kunst and V. Dwivedi, *Phys. Rev. B* **99**, 245116 (2019).
- [34] S. Longhi, *Phys. Rev. Lett.* **122**, 237601 (2019).
- [35] E. Edvardsson, F. K. Kunst, and E. J. Bergholtz, *Phys. Rev. B* **99**, 081302(R) (2019).
- [36] K. Kawabata, K. Shiozaki, M. Ueda, and M. Sato, *Phys. Rev. X* **9**, 041015 (2019).
- [37] H. Zhou and J. Y. Lee, *Phys. Rev. B* **99**, 235112 (2019).
- [38] L. Herviou, J. H. Bardarson, and N. Regnault, *Phys. Rev. A* **99**, 052118 (2019).
- [39] Q.-B. Zeng, Y.-B. Yang, and Y. Xu, *Phys. Rev. B* **101**, 020201(R) (2020).
- [40] M. R. Hirsbrunner, T. M. Philip, and M. J. Gilbert, *Phys. Rev. B* **100**, 081104(R) (2019).
- [41] H.-G. Zirnstein, G. Refael, and B. Rosenow, *Phys. Rev. Lett.* **126**, 216407 (2021).
- [42] S. R. Pocock, P. A. Huidobro, and V. Giannini, *Nanophotonics* **8**, 1337 (2019).
- [43] K. Kimura, T. Yoshida, and N. Kawakami, *Phys. Rev. B* **100**, 115124 (2019).
- [44] D. S. Borgnia, A. J. Kruchkov, and R.-J. Slager, *Phys. Rev. Lett.* **124**, 056802 (2020).
- [45] K. Kawabata, T. Bessho, and M. Sato, *Phys. Rev. Lett.* **123**, 066405 (2019).
- [46] K. Yokomizo and S. Murakami, *Phys. Rev. Lett.* **123**, 066404 (2019).
- [47] F. Song, S. Yao, and Z. Wang, *Phys. Rev. Lett.* **123**, 246801 (2019).
- [48] P. A. McClarty and J. G. Rau, *Phys. Rev. B* **100**, 100405(R) (2019).
- [49] N. Okuma and M. Sato, *Phys. Rev. Lett.* **123**, 097701 (2019).
- [50] F. Song, S. Yao, and Z. Wang, *Phys. Rev. Lett.* **123**, 170401 (2019).
- [51] E. J. Bergholtz and J. C. Budich, *Phys. Rev. Res.* **1**, 012003(R) (2019).
- [52] J. Y. Lee, J. Ahn, H. Zhou, and A. Vishwanath, *Phys. Rev. Lett.* **123**, 206404 (2019).
- [53] C.-X. Guo, X.-R. Wang, C. Wang, and S.-P. Kou, *Phys. Rev. B* **101**, 144439 (2020).
- [54] T. Yoshida, K. Kudo, and Y. Hatsugai, *Sci. Rep.* **9**, 16895 (2019).
- [55] W. B. Rui, M. M. Hirschmann, and A. P. Schnyder, *Phys. Rev. B* **100**, 245116 (2019).

- [56] W. Brzezicki and T. Hyart, *Phys. Rev. B* **100**, 161105(R) (2019).
- [57] H. Schomerus, *Phys. Rev. Res.* **2**, 013058 (2020).
- [58] K.-I. Imura and Y. Takane, *Phys. Rev. B* **100**, 165430 (2019).
- [59] L. Herviou, N. Regnault, and J. H. Bardarson, *SciPost Phys.* **7**, 069 (2019).
- [60] P.-Y. Chang, J.-S. You, X. Wen, and S. Ryu, *Phys. Rev. Res.* **2**, 033069 (2020).
- [61] X.-X. Zhang and M. Franz, *Phys. Rev. Lett.* **124**, 046401 (2020).
- [62] K. Zhang, Z. Yang, and C. Fang, *Phys. Rev. Lett.* **125**, 126402 (2020).
- [63] Z. Yang, K. Zhang, C. Fang, and J. Hu, *Phys. Rev. Lett.* **125**, 226402 (2020).
- [64] N. Okuma, K. Kawabata, K. Shiozaki, and M. Sato, *Phys. Rev. Lett.* **124**, 086801 (2020).
- [65] S. Longhi, *Phys. Rev. Lett.* **124**, 066602 (2020).
- [66] X.-R. Wang, C.-X. Guo, and S.-P. Kou, *Phys. Rev. B* **101**, 121116(R) (2020).
- [67] N. Matsumoto, K. Kawabata, Y. Ashida, S. Furukawa, and M. Ueda, *Phys. Rev. Lett.* **125**, 260601 (2020).
- [68] T. Yoshida, T. Mizoguchi, and Y. Hatsugai, *Phys. Rev. Res.* **2**, 022062 (2020).
- [69] K. Yokomizo and S. Murakami, *Phys. Rev. Res.* **2**, 043045 (2020).
- [70] L. Li, C. H. Lee, S. Mu, and J. Gong, *Nat. Commun.* **11**, 5491 (2020).
- [71] K. Kawabata, N. Okuma, and M. Sato, *Phys. Rev. B* **101**, 195147 (2020).
- [72] F. Terrier and F. K. Kunst, *Phys. Rev. Res.* **2**, 023364 (2020).
- [73] T. Bessho and M. Sato, *Phys. Rev. Lett.* **127**, 196404 (2021).
- [74] J. Claes and T. L. Hughes, *Phys. Rev. B* **103**, L140201 (2021).
- [75] H.-G. Zirnstein and B. Rosenow, *Phys. Rev. B* **103**, 195157 (2021).
- [76] M. M. Denner, A. Skurativska, F. Schindler, M. H. Fischer, R. Thomale, T. Bzdušek, and T. Neupert, *Nat. Commun.* **12**, 5681 (2021).
- [77] R. Okugawa, R. Takahashi, and K. Yokomizo, *Phys. Rev. B* **102**, 241202(R) (2020).
- [78] K. Kawabata, M. Sato, and K. Shiozaki, *Phys. Rev. B* **102**, 205118 (2020).
- [79] Y. Fu, J. Hu, and S. Wan, *Phys. Rev. B* **103**, 045420 (2021).
- [80] N. Okuma and M. Sato, *Phys. Rev. B* **103**, 085428 (2021).
- [81] K. Kawabata, K. Shiozaki, and S. Ryu, *Phys. Rev. Lett.* **126**, 216405 (2021).
- [82] Y. Yi and Z. Yang, *Phys. Rev. Lett.* **125**, 186802 (2020).
- [83] K. Zhang, Z. Yang, and C. Fang, *Nat. Commun.* **13**, 2496 (2022).
- [84] X.-Q. Sun, P. Zhu, and T. L. Hughes, *Phys. Rev. Lett.* **127**, 066401 (2021).
- [85] K. Shiozaki and S. Ono, *Phys. Rev. B* **104**, 035424 (2021).
- [86] R. Okugawa, R. Takahashi, and K. Yokomizo, *Phys. Rev. B* **103**, 205205 (2021).
- [87] P. M. Vecsei, M. M. Denner, T. Neupert, and F. Schindler, *Phys. Rev. B* **103**, L201114 (2021).
- [88] H. Hu, E. Zhao, and W. V. Liu, *Phys. Rev. B* **106**, 094305 (2022).
- [89] A. K. Ghosh and T. Nag, *Phys. Rev. B* **106**, L140303 (2022).
- [90] C. Poli, M. Bellec, U. Kuhl, F. Mortessagne, and H. Schomerus, *Nat. Commun.* **6**, 6710 (2015).
- [91] J. M. Zeuner, M. C. Rechtsman, Y. Plotnik, Y. Lumer, S. Nolte, M. S. Rudner, M. Segev, and A. Szameit, *Phys. Rev. Lett.* **115**, 040402 (2015).
- [92] B. Zhen, C. W. Hsu, Y. Igarashi, L. Lu, I. Kaminer, A. Pick, S.-L. Chua, J. D. Joannopoulos, and M. Soljačić, *Nature (London)* **525**, 354 (2015).
- [93] S. Weimann, M. Kremer, Y. Plotnik, Y. Lumer, S. Nolte, K. G. Makris, M. Segev, M. C. Rechtsman, and A. Szameit, *Nat. Mater.* **16**, 433 (2017).
- [94] L. Xiao, X. Zhan, Z. H. Bian, K. K. Wang, X. Zhang, X. P. Wang, J. Li, K. Mochizuki, D. Kim, N. Kawakami, W. Yi, H. Obuse, B. C. Sanders, and P. Xue, *Nat. Phys.* **13**, 1117 (2017).
- [95] P. St-Jean, V. Goblot, E. Galopin, A. Lemaître, T. Ozawa, L. L. Gratiet, I. Sagnes, J. Bloch, and A. Amo, *Nat. Photonics* **11**, 651 (2017).
- [96] M. Parto, S. Wittek, H. Hodaei, G. Harari, M. A. Bandres, J. Ren, M. C. Rechtsman, M. Segev, D. N. Christodoulides, and M. Khajavikhan, *Phys. Rev. Lett.* **120**, 113901 (2018).
- [97] B. Bahari, A. Ndao, F. Vallini, A. E. Amili, Y. Fainman, and B. Kanté, *Science* **358**, 636 (2017).
- [98] H. Zhao, P. Miao, M. H. Teimourpour, S. Malzard, R. El-Ganainy, H. Schomerus, and L. Feng, *Nat. Commun.* **9**, 981 (2018).
- [99] H. Zhou, C. Peng, Y. Yoon, C. W. Hsu, K. A. Nelson, L. Fu, J. D. Joannopoulos, M. Soljačić, and B. Zhen, *Science* **359**, 1009 (2018).
- [100] G. Harari, M. A. Bandres, Y. Lumer, M. C. Rechtsman, Y. D. Chong, M. Khajavikhan, D. N. Christodoulides, and M. Segev, *Science* **359**, eaar4003 (2018).
- [101] M. A. Bandres, S. Wittek, G. Harari, M. Parto, J. Ren, M. Segev, D. Christodoulides, and M. Khajavikhan, *Science* **359**, eaar4005 (2018).
- [102] A. Cerjan, S. Huang, K. P. Chen, Y. Chong, and M. C. Rechtsman, *Nat. Photonics* **13**, 623 (2019).
- [103] H. Zhao, X. Qiao, T. Wu, B. Midya, S. Longhi, and L. Feng, *Science* **365**, 1163 (2019).
- [104] M. Brandenbourger, X. Locsin, and C. C. E. Lerner, *Nat. Commun.* **10**, 4608 (2019).
- [105] A. Ghatak, M. Brandenbourger, J. Van Wezel, and C. Coulais, *Proc. Natl. Acad. Sci. U.S.A.* **117**, 29561 (2020).
- [106] T. Helbig, T. Hofmann, S. Imhof, M. Abdelghany, T. Kiessling, L. Molenkamp, C. Lee, A. Szameit, M. Greiter, and R. Thomale, *Nat. Phys.* **16**, 747 (2020).
- [107] T. Hofmann, T. Helbig, F. Schindler, N. Salgo, M. Brzezińska, M. Greiter, T. Kiessling, D. Wolf, A. Vollhardt, A. Kabaši, C. H. Lee, A. Bilušić, R. Thomale, and T. Neupert, *Phys. Rev. Res.* **2**, 023265 (2020).
- [108] L. Xiao, T. Deng, K. Wang, G. Zhu, Z. Wang, W. Yi, and P. Xue, *Nat. Phys.* **16**, 761 (2020).

- [109] S. Weidemann, M. Kremer, T. Helbig, T. Hofmann, A. Stegmaier, M. Greiter, R. Thomale, and A. Szameit, *Science* **368**, 311 (2020).
- [110] K. Wang, A. Dutt, K. Y. Yang, C. C. Wojcik, J. Vučković, and S. Fan, *Science* **371**, 1240 (2021).
- [111] W. Zhang, X. Ouyang, X. Huang, X. Wang, H. Zhang, Y. Yu, X. Chang, Y. Liu, D.-L. Deng, and L.-M. Duan, *Phys. Rev. Lett.* **127**, 090501 (2021).
- [112] X. Zhang, Y. Tian, J.-H. Jiang, M.-H. Lu, and Y.-F. Chen, *Nat. Commun.* **12**, 5377 (2021).
- [113] D. Zou, T. Chen, W. He, J. Bao, C. H. Lee, H. Sun, and X. Zhang, *Nat. Commun.* **12**, 7201 (2021).
- [114] L. S. Palacios, S. Tchoumakov, M. Guix, I. Pagonabarraga, S. Sánchez, and A. G. Grushin, *Nat. Commun.* **12**, 4691 (2021).
- [115] K. Wang, A. Dutt, C. C. Wojcik, and S. Fan, *Nature (London)* **598**, 59 (2021).
- [116] Y. Hatsugai, *Phys. Rev. Lett.* **71**, 3697 (1993).
- [117] L.-Z. Tang, L.-F. Zhang, G.-Q. Zhang, and D.-W. Zhang, *Phys. Rev. A* **101**, 063612 (2020).
- [118] H. Liu, Z. Su, Z.-Q. Zhang, and H. Jiang, *Chin. Phys. B* **29**, 050502 (2020).
- [119] H. Liu, J.-K. Zhou, B.-L. Wu, Z.-Q. Zhang, and H. Jiang, *Phys. Rev. B* **103**, 224203 (2021).
- [120] Sayed Ali Akbar Ghorashi, T. Li, M. Sato, and T. L. Hughes, *Phys. Rev. B* **104**, L161116 (2021).
- [121] Sayed Ali Akbar Ghorashi, T. Li, and M. Sato, *Phys. Rev. B* **104**, L161117 (2021).
- [122] Skin modes are obtained using GBZ and thus bulk modes [18], while surface states are not obtained using GBZ and thus not bulk modes.
- [123] I. Mondragon-Shem, T. L. Hughes, J. Song, and E. Prodan, *Phys. Rev. Lett.* **113**, 046802 (2014).
- [124] J. Song and E. Prodan, *Phys. Rev. B* **89**, 224203 (2014).
- [125] E. Prodan and H. Schulz-Baldes, *J. Funct. Anal.* **271**, 1150 (2016).
- [126] H. Katsura and T. Koma, *J. Math. Phys. (N.Y.)* **59**, 031903 (2018).
- [127] J. Bellissard, A. van Elst, and H. Schulz-Baldes, *J. Math. Phys. (N.Y.)* **35**, 5373 (1994).
- [128] A. Y. Kitaev, *Ann. Phys. (N.Y.)* **321**, 2 (2006).
- [129] Note that the isotropic structure of $\mp e^{\pm ik_y}$ in the complex energy plane causes highly degenerated in-gap skin modes at $E = 0$.
- [130] See Supplemental Material at <http://link.aps.org/supplemental/10.1103/PhysRevLett.132.136401>, which includes Refs. [131–134], for a demonstration of how the real-space 3D winding number changes with different boundary conditions, a proof of the BBC for point-gap topological phases in all 38-fold symmetry classes, and a connection between intrinsic point-gap topological phases in the OBC and a single exceptional point.
- [131] E. Prodan, T. L. Hughes, and B. A. Bernevig, *Phys. Rev. Lett.* **105**, 115501 (2010).
- [132] H. Katsura and T. Koma, *J. Math. Phys. (N.Y.)* **57**, 021903 (2016).
- [133] Y. Akagi, H. Katsura, and T. Koma, *J. Phys. Soc. Jpn.* **86**, 123710 (2017).
- [134] Z. Yang, A. P. Schnyder, J. Hu, and C.-K. Chiu, *Phys. Rev. Lett.* **126**, 086401 (2021).
- [135] T. Yoshida, R. Peters, N. Kawakami, and Y. Hatsugai, *Prog. Theor. Exp. Phys.* **2020**, 12A109 (2020).
- [136] X.-L. Qi, T. L. Hughes, and S.-C. Zhang, *Phys. Rev. B* **78**, 195424 (2008).